Dynamic Performance of a Wind Turbine Based on a Self-Excited Induction Generator

Allal. M BOUZID[1, 2]   Ahmed CHERITI[1]   Alex HUGGETT[2]

1 Département of Computer and Electrical Engineering, Université du Québec à Trois-Rivières, Canada
2 Opal-RT Technologies, Montréal, QC H3K 1G6, CANADA

Abstract
The paper is devoted to the study of the dynamic performance of a wind turbine in a remote site microgrid based on a self-excited induction generator (SEIG) during sudden load connection. A dynamic model of the currents of the SEIG in the stationary reference frame dq axis is introduced and the main effect of saturation flux in the SEIG is explained. The case of self-excitation with different capacities and connected with purely resistive and inductive loads are discussed in this paper.
Keywords: Renewable Energy, Induction Generator, Islanded Wind, Modeling, Self-Excited Induction Generator

Nomenclature

V_{ds}, V_{dr}	: Stator, rotor d-axis voltages
I_{ds}, I_{dr}	: Stator, rotor d-axis currents
V_{qs}, V_{qr}	: Stator, rotor q-axis voltages
I_{qs}, I_{qr}	: Stator, rotor q-axis currents
L_m	: Magnetizing Inductance
L_s, L_r	: Stator, Rotor Inductances
I_m	: Magnetizing current
T_e	: Electromagnetic Torque
P	: Number of poles
R_s, R_r	: Stator, Rotor resistance
C_{dq}	:Per phase terminal excitation capacitance
R, L	: Load Resistance/ Inductance per phase
ω_r	: Angular speeds of Rotor
V_{ld}, V_{lq}	: d-q axes load voltage per phase
I_{ld}, I_{lq}	: d-q axes load current per phase
V_{cd}, V_{cq}	: d-q axes capacitor voltage per phase
I_{cd}, I_{cq}	: d-q axes capacitor currents per phase
T_{shaft}	: Shaft load torque.
X	: Multiplier of speed
P_{aer}	: The mechanical input power
V_w	: Wind velocity
β	: Blade angle
R_w	: Radius of the wind turbine
ρ	: Air density

1. Introduction

The gradual increase in oil prices combined with the hope to reduce oil consumption over the next 50 years have forced researchers to focus their attention to the production of green electricity as an alternative power source [1]. The self-excited induction generators are good candidates for application in wind turbines in remote areas, because they do not need an external power supply to produce their magnetic field [2]. These generators are very important because of their convenience for various applications in the field of green electricity production [3]. The permanent magnet generators can also be used for wind energy applications but suffer from an uncontrollable magnetic field, which degrades over a period due to the weakening of magnets, and the voltage produced tends to fall steeply with the load. FIG. 1 shows the principle of converting electric energy in a wind turbine. The SEIG has a self-protection mechanism because the voltage collapses when there is a short circuit at its terminals. In addition, SEIGs have other advantages such as low cost, reduced maintenance, brushless construction with the squirrel cage rotor and simple, no DC power required for excitation. The cost of maintenance is low cost compared to the synchronous generator [3, 4].
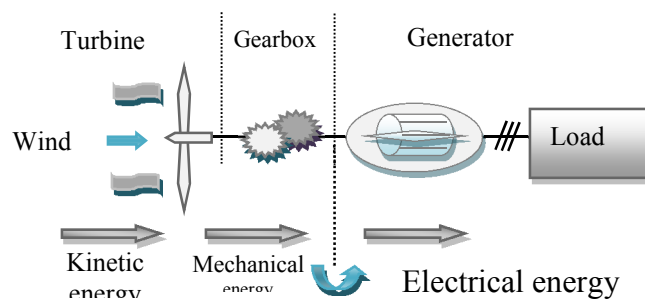
Fig. 1. Principles of Wind Energy Conversion

2. Modeling of Wind Turbine

2.1 Aerodynamic Model

The aerodynamic model should produce aerodynamic torque from the wind speed and the rotational speed of the turbine. This speed corresponds to the rotational speed of the low-speed shaft (Ωb) [5, 6]. To perform modeling of aerodynamics, the expression of mechanical power produced by a wind turbine is used. This quantity of power P_{aer} depends on the C_p power coefficient. It is given by the following equation:

$$P_{aer} = \frac{1}{2}\rho\pi R^2 V^3 C_p(\lambda,\beta) \qquad (1)$$

The power coefficient is a function of the specific speed (λ) and the pitch angle (β) of the blades of the wind turbine. The expression of mechanical power can be modified to represent the mechanical torque of the power extracted from the wind:

$$T_{aer} = \frac{1}{2}\rho\pi R^2 V^3 \frac{C_p(\lambda,\beta)}{\Omega_b} \qquad (2)$$

$$\lambda = \frac{\Omega_b R}{V} \qquad (3)$$

If β is fixed, we have:

$$T_{aer} = \frac{1}{2}\rho\pi R^2 V^3 \frac{C_p(\lambda)}{\Omega_b} \qquad (4)$$

The power coefficient is generally modeled by the following analytical expression:

$$C_p(\lambda,\beta) = c_1\left(\frac{c_2}{\lambda_i} - c_3\beta - c_4\right)e^{\frac{-c_5}{\lambda_i}} + c_6\lambda \qquad (5)$$

$$\lambda_i = \left(\frac{1}{\lambda+0.08\beta} - \frac{0.035}{\beta^3+1}\right)^{-1} \qquad (6)$$

With $c_1 = 0.5176, c_2 = 116, c_3 = 0.4, c_4 = 5, \ c_5 = 21, c_6 = 0.0068$

A typical ratio of C_p and λ is shown in Fig.2. It is clear from this figure that there is a λ value for which the power coefficient (C_p) is maximized [6].
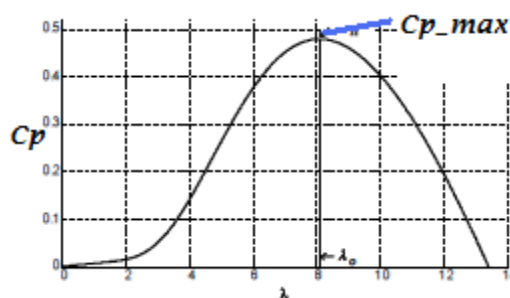
Fig. 2. Power coefficient in function of the specific speed for a fixed pitch (β = 0)

2.2 Wind Speed Gearbox Model

The multiplier adjusts the speed (slow) of the turbine to the generator speed in Fig. 3. This multiplier is mathematically modeled by the following equations

$$T_D = T_{aer}/G \qquad (7)$$

$$\Omega_{turbine} = \frac{\Omega_{mec}}{G} \qquad (8)$$
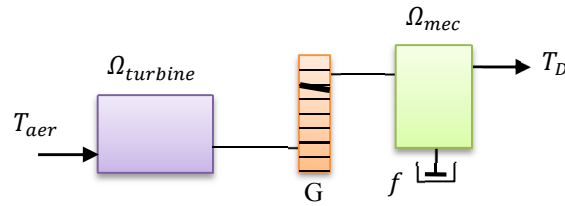
Fig. 3. Simplified mechanical model of the turbine

3. Modeling of SEIG

The model used for the simulation of the operation of the asynchronous machine takes into account the effect of saturation of the materials. Indeed, the gap of asynchronous machines is generally low and the nonlinearity of magnetic materials has a significant effect [7, 8] This effect is difficult to understand in the case of conventional phase models. Therefore, it usually adopts two-phase models to consider in a comprehensive manner. Of course, this assumes that the induction is homogeneous in the whole structure. In our approach, we adopt the model of Park d-q of the asynchronous machine. The effect of saturation is taken into account via a magnetizing inductance (L_m). This is approximated by a polynomial function of the voltage V_{ph} [8, 9]. Using the relationships between the components of flux and currents in the dq arbitrary reference benchmark yields the voltage equations and flow expressed as:

3.1 Electrical Equation

To the stator

$$\begin{cases} V_{qs} = R_s i_{qs} + \omega \phi_{ds} + p\phi_{qs} \\ V_{ds} = R_s i_{ds} - \omega \phi_{qs} + p\phi_{ds} \end{cases} \tag{9}$$

To the rotor

$$\begin{cases} V'_{qr} = R'_r i'_{qr} + (\omega - \omega_r)\phi'_{dr} + p\phi'_{qr} \\ V'_{dr} = R'_r i'_{dr} - (\omega - \omega_r)\phi'_{qr} + p\phi'_{dr} \end{cases} \tag{10}$$

3.2 Magnetic Equation

To the stator:

$$\begin{cases} \phi_{qs} = L_{ls} i_{qs} + L_m(i_{qs} + i'_{qr}) \\ \phi_{ds} = L_{ls} i_{ds} + L_m(i_{ds} + i'_{dr}) \end{cases} \tag{11}$$

To the rotor:

$$\begin{cases} \phi'_{qr} = L'_{lr} i'_{qr} + L_m(i_{qs} + i'_{qr}) \\ \phi'_{dr} = L'_{lr} i'_{dr} + L_m(i_{ds} + i'_{dr}) \end{cases} \tag{12}$$

3.3 Equation of electromagnetic torque:

$$T_e = \left(\frac{3}{2}\right)(PL_m)\left(i_{ds} i'_{qr} - i_{qs} i'_{dr}\right) \tag{13}$$

3.4 Driving torque of the SEIG:

$$T_D = \left(\frac{J}{P}\right) P\omega_r + T_e + fP\omega_r \tag{14}$$

$$\Omega_{mec} = P.\omega_r \tag{15}$$

Where ϕ_{qs}, ϕ_{ds}, ϕ'_{dr} and ϕ'_{qr} denotes the flux linkage, $p = d/dt$ denotes Laplace transformation.

The self-excited induction generator (SEIG) works just like an induction machine in the saturation region, except for the fact that there are excitation capacitors connected across the terminals of the stator. In our work, the benchmark reference related to the stator ($\omega = 0$) is used to simulate the model of SEIG Fig. 4

(a)

(b)
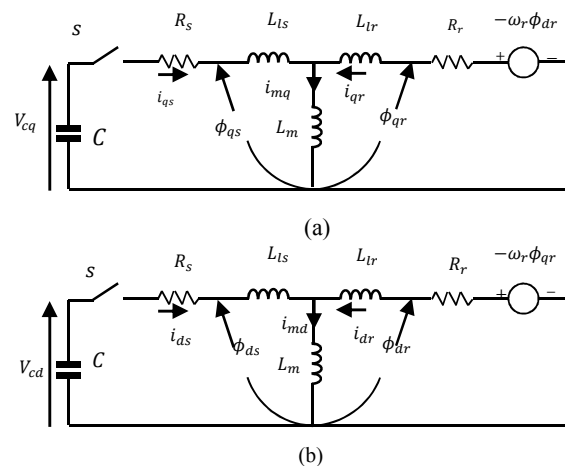
Fig. 4. Circuit diagrams of the SEIG in the Park reference d-axis and q-axis connected to the stator
State-space dynamic model of SEIG

$$\dot{I} = AI + B \tag{16}$$

$$\begin{cases} I = \begin{bmatrix} i_{qs} \\ i_{ds} \\ i_{qr} \\ i_{dr} \end{bmatrix} \quad B = \frac{1}{L} \begin{bmatrix} L_m K_{qr} - L_r V_{cq} \\ L_m K_{dr} - L_r V_{cd} \\ L_m V_{cq} - L_s K_{qr} \\ L_m V_{cd} - L_s K_{dr} \end{bmatrix} \\[2em] A = \frac{1}{L} \begin{bmatrix} -L_r R_s & -L_m^2 \omega_r & L_m R_r & -L_m \omega_r L_r \\ L_m^2 \omega_r & -L_s R_s & L_m \omega_r L_r & L_m R_r \\ L_m R_s & L_s \omega_r L_m & -L_s R_r & L_s \omega_r L_r \\ -L_s \omega_r L_m & L_m R_s & -L_s \omega_r L_r & -L_s R_r \end{bmatrix} \end{cases} \tag{17}$$

$$L_s = L_{ls} + L_m \ \text{et} \ L_r = L_{lr} + L_m \tag{18}$$

The capacitor voltages in Fig. 4 can be represented:

$$V_{cq} = \frac{1}{C} \int i_{qs}\, dt + V_{cq0} \tag{19}$$

$$V_{cd} = \frac{1}{C} \int i_{ds}\, dt + V_{cd0} \tag{20}$$

3.5 Determination of the initial conditions
The induction machine requires the residual magnetism for the self-energizing process. Residual magnetism cannot be zero. The initial conditions required in the equation for the simulation of self-excited induction generator can be determined from measurements of the induction machine and capacitors. The initial voltage on the capacitor decreases with time due to leaks. V_{cq0}, V_{cd0} are the initial capacitor voltages.

$$V_{cq0} = V_{cq}\big|_{t=0} \ \text{et} \ V_{cd0} = V_{cd}\big|_{t=0} \tag{21}$$

The constants K_{dr} and K_{qr} are due to the remanent flux in the machine.

$$K_{dr} = \omega_r \phi_{qr0} \ \text{et} \ K_{qr} = \omega_r \phi_{dr0}. \tag{22}$$

3.6 Modeling of an Autonomous Induction Generator Taking Into Account the Saturation
In most cases, the linear model of the asynchronous machine is sufficient to achieve good results in the analysis of transients (start ...). This model assumes that the magnetizing inductance is constant, which is not entirely true, since the magnetic material used for manufacturing is not perfectly linear. However, in certain uses of the asynchronous machine (self-excited generator, wind), it is essential to take account of the effect of saturation of the magnetic circuit and thus the variation of the magnetizing inductance [10, 11]. When the capacitors are connected across the terminals of the stator of an induction machine, driven by an external motor or a wind turbine, a voltage will be induced on its terminals. The electromotive force (EMF) and the current induced in the stator windings will continue to rise until the balanced state is reached, influenced by the magnetic saturation of the

machine. Therefore, the magnetizing current should be calculated for each stage of integration in terms of dq currents of the stator and rotor as:

$$I_m = \sqrt{(I_{ds} + I_{dr})^2 + (I_{qs} + I_{qr})^2} \qquad (23)$$

$$I_m = \sqrt{(V_{ds})^2 + (V_{qs})^2} \qquad (24)$$

The magnetizing inductance is calculated from the magnetization characteristic expressed using the curve between Lm and V_{ph}. The relationship between Lm and V_{ph} is achieved by a synchronous speed test for SEIG testing and can be written as:

$$L_m = -1.57 \times 10^{-11}V_{ph}^2 + 2.44 \times 10^{-8}V_{ph}^3 - 1.19 \times 10^{-5}V_{ph}^2 + 1.42 \times 10^{-3}V_{ph} + 0.245 \quad (25)$$

TABLE.1. PARAMETERS OF THE TURBINE.

Parameters name	Values
Wind radius	R=35.25 m
Multiplier Gain	G = 6
Inertia of the shaft	J =100 kg.m^2
Air density	ρ =1.225 kg/m^3

TABLE.2. PARAMETERS OF THE SEIG.

Parameters name	Values
Nominal power	P_m = 3.6 KW
Nominal voltage	V_n=250 V (Δ)
Nominal current	I_n =7.8 A
Stator resistance	R_s = 1.66 Ω
Rotor resistance	R_r = 2.74 Ω
Stator inductance	L_s = 11.4 mH
Rotor inductance	L_r = 11.4 mH
Mutual inductance	L_m= 180 mH
Number of pole pairs	P = 2
Coefficient of friction	f_r=0.0024N.m.s^{-1}
Frequency	F = 50 Hz

4. Simulation Results

Simulation results were determined for the SEIG without load and different loads, with the conditions of balanced and unbalanced excitation. The simulations were obtained with MATLAB / Simulink. Residual magnetism in the machine is taken into account in the simulation process, since it is necessary for the self-excitation. The data of this machine are given in Table no.1 and no.2 Table. The performance of this machine has been studied in different conditions, being balanced and unbalanced. Two excitation capacitors are chosen for $C_d = C_q = 60\ \mu F$.
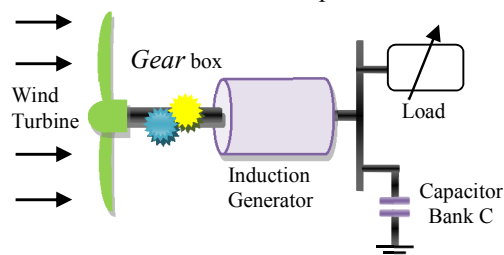
Fig. 5. Schematic Diagram of the WECS
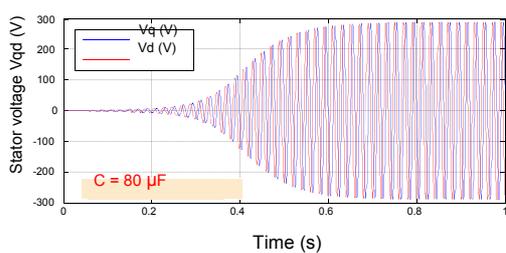
a. Stator voltage for $C_q = C_q = 80 \ \mu F$
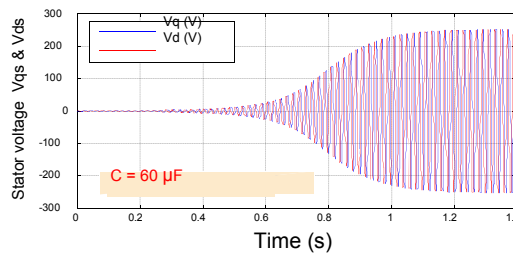
b. Stator voltage for $C_q = C_q = 60 \ \mu F$
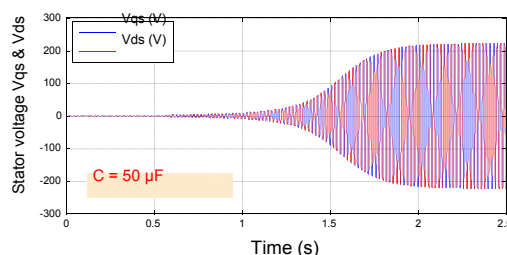
c. Stator voltage for $C_q = C_q = 50 \ \mu F$

Fig. 6. Voltage accumulation under different capacitors excitation
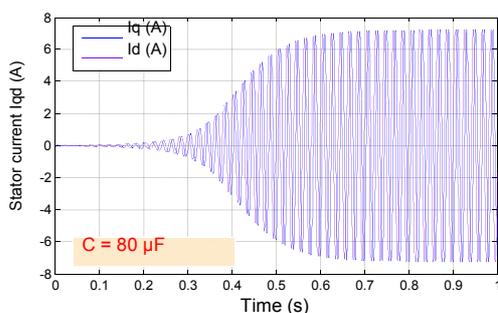
a. Stator current for $C_q = C_q = 80 \ \mu F$
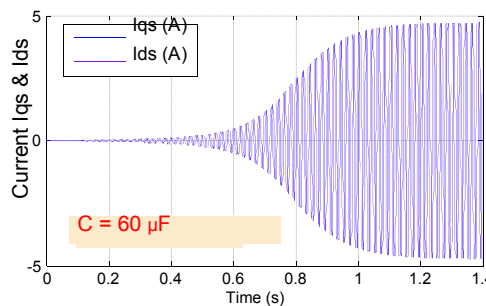
b. Stator current for $C_q = C_q = 60 \ \mu F$
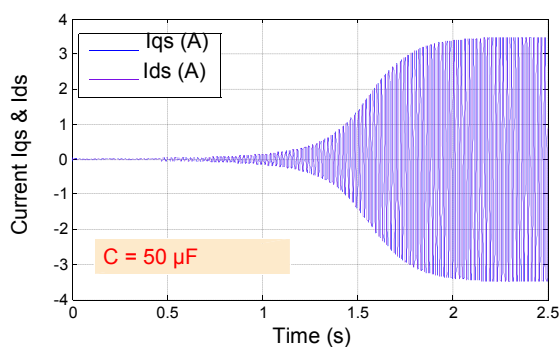
c. Stator current for $C_q = C_q = 50 \ \mu F$

Fig. 7. Current accumulation under different capacitors excitation

The passenger response to different excitation capacitors Fig.6 shows the voltage accumulation under different capacitors excitement. It is clear that the process of accumulation is much faster with the larger capacitor ($80 \ uF$). In addition, the importance of voltage is much higher in the case of larger capacitor. The effect of the excitation capacitor on the generator current is illustrated in Fig.7. The excitation current is higher with the larger capacitor excitation.

4.1 Sudden loss of a portion of excitation capacitor in a phase
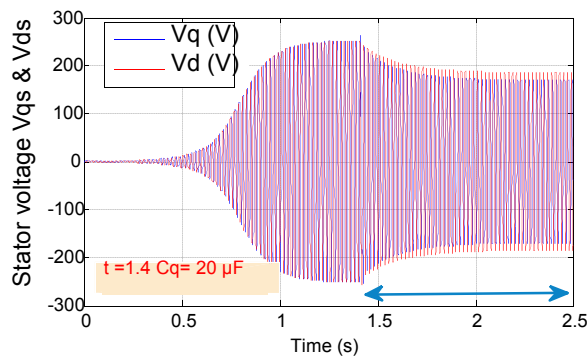
Fig. 8. Voltage curve with a loss of part of the excitation capacitor
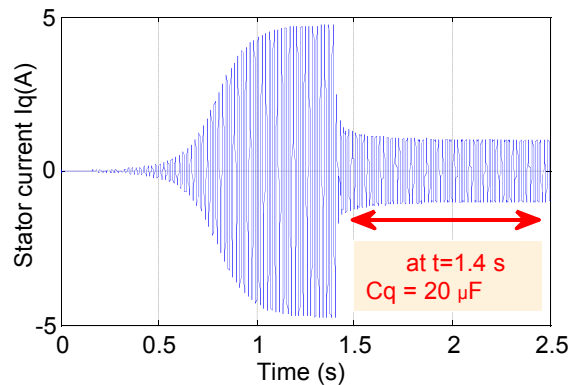
a.   Stator current Iq
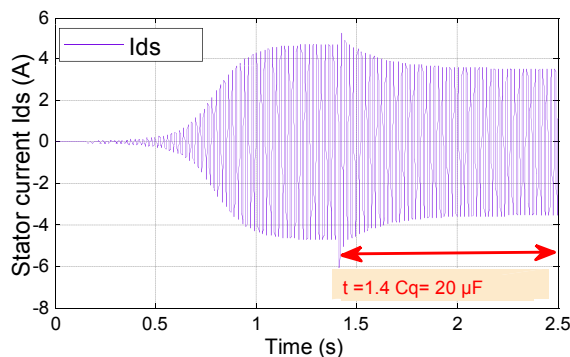
b.   Stator current Id

Fig. 9. Current curve with a loss of a part of the excitation capacitor

Fig. 8 shows the response of the SEIG when there is a sudden loss of an excitation capacitor. It is assumed that the phase excitation capacitor V_{sq} suddenly changed C_q $from$ 60 to $50\mu F$ at t = 1.4 seconds while C_d is kept without change. This case represents an imbalance upon excitation of the SEIG. It is clear that this disruption reduces the phase voltages differently. The effect of the disturbance on the phase current is shown in Fig.9. The reduction of the excitation capacitor could lead to voltage collapse as can be seen in Fig.8.

4.2 Simulation of self-priming in a resistive load.

The principle is the same as empty, except that the additional equations will change as follows:

$$\begin{cases} i_c = i_s - i_l \\ \frac{dV_c}{dt} = \frac{1}{C} i_c \\ i_l = \frac{V_c}{R} \end{cases} \tag{26}$$

i_{ch}: load current.
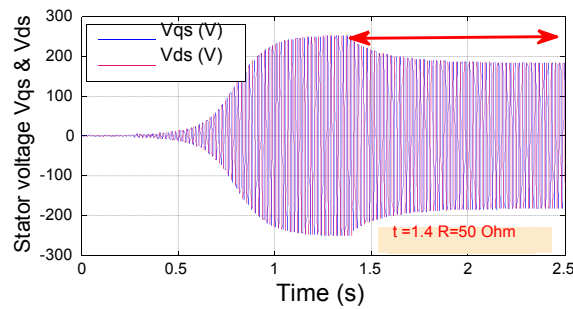
Fig. 10. Voltage curve with a resistive load R
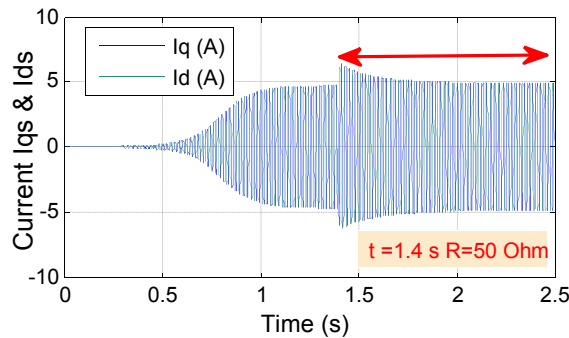
Fig. 11. Current curve with a resistive load R
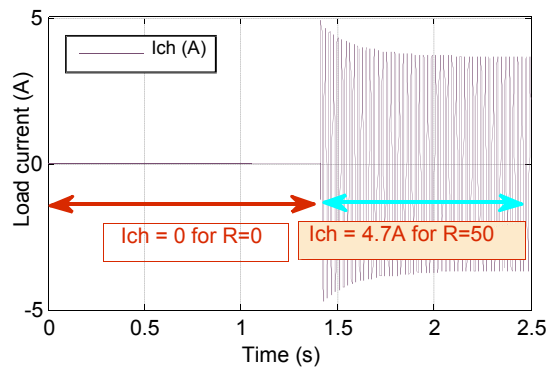
Fig. 12. Current curve of the resistive load R
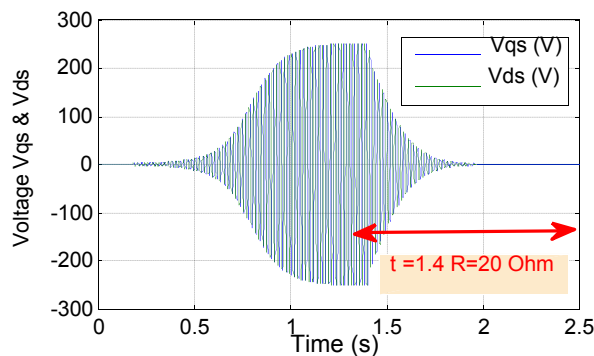
Fig. 13. Voltage curve for resistive load R=20Ω

The effect of the sudden change by a resistive load is shown in Fig.10. Fig.10. At $t = 1.4$ seconds the resistive load of 50Ω value is suddenly applied across each phase. It is clear that the voltage drop and current increases with an increase against Fig.12 load current. But when applying a load $R = 20\Omega$ is clearly seen on Fig.13 and Fig. 14, the SEIG peaks and the excitation capacitor cannot have the means for balanced operation and the generator loses its voltage.
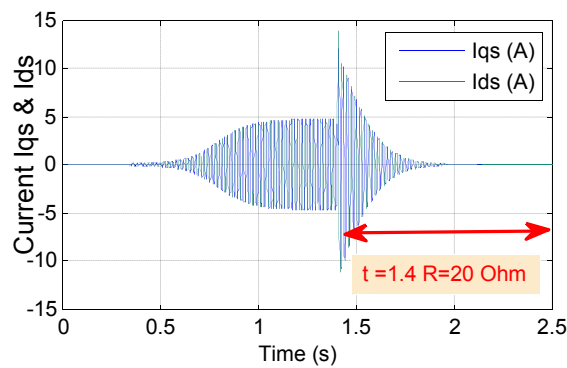
Fig. 14. Current curve for resistive load R = 20Ω

4.3 Simulation of self-priming with an inductive load.

The principle of self-priming charge remains the same as no load, except that the equations of excitement will take another form. The equations in the generalized reference Park transform are:

$$\begin{cases} \frac{d}{dt}V_{ds} = \frac{1}{C}(i_{ds} - i_{ld}) \\ \frac{d}{dt}i_{ld} = \frac{1}{L_{ch}}(V_{ds} - R_l i_{ld}) \end{cases} \tag{27}$$

$$\begin{cases} \frac{d}{dt}V_{qs} = \frac{1}{C}(i_{qs} - i_{lq}) \\ \frac{d}{dt}i_{lq} = \frac{1}{L_l}(V_{qs} - R_l i_{lq}) \end{cases} \tag{28}$$
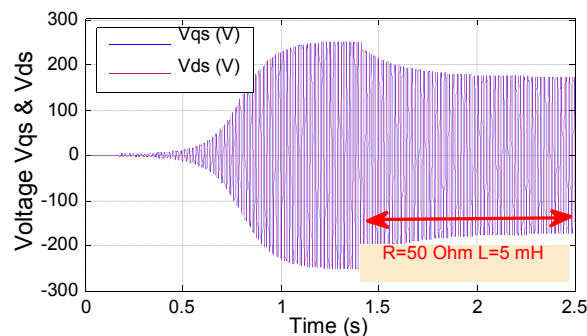
Fig. 15. Voltage curve for RL load
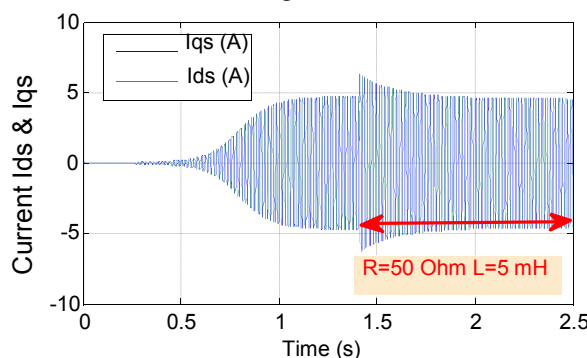
Fig. 16. Current curve for RL load

The effect of the sudden change by RL load is shown in Fig.15. Fig.16. At $t = 1.4$ seconds where $R = 50\Omega$ and $L = 5\,mH$ is suddenly applied across each phase. It is clear that the voltage drop and current increases with an increase against Fig.17 load current.

9
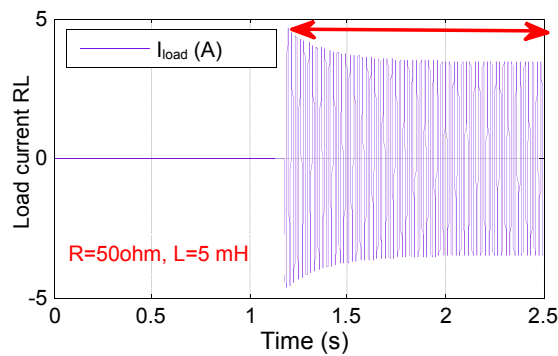
Fig. 17. Current curve of the RL load
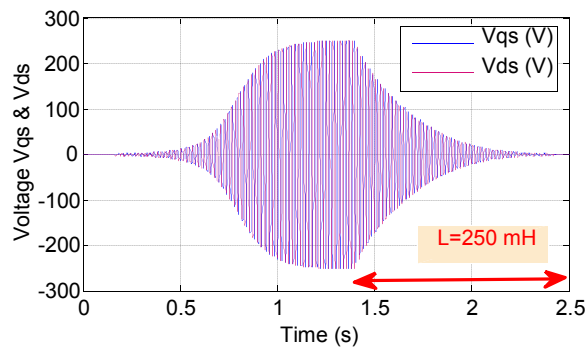
Fig. 18. Voltage curve for purely inductive load
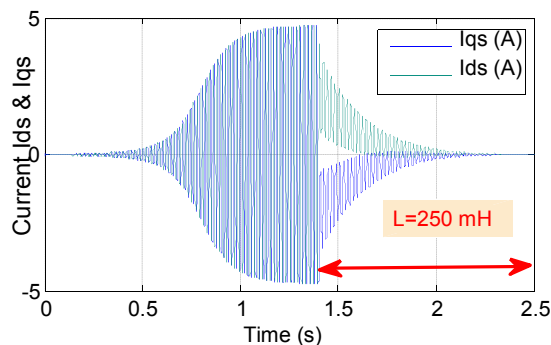
Fig. 19. Current curve for purely inductive load

The effect of a pure inductive load on transient response is seen in Fig.18 and Fig.19, when a sudden pure inductive load is applied at $t = 1.4\ seconds$. The inductor value applied through each phase is $250\ mH$. The response indicates that the excitation capacitors are not in this case able to keep a stable operation.

Conclusion

This model is suitable for studying the generator operation in balanced and unbalanced conditions. Operating the generator to different values of the excitation capacitors is studied in this paper, and the results indicate that the high voltages correspond with high values of the excitation capacitors. Disconnecting a part of the excitation capacitors in a phase may lead to voltage collapse as shown by the results. The application of the resistive load can also lead to a complete loss of output voltage if it exceeds certain limits, which can have an indirect effect on the excitation current. The increase in the inductive load reduces the output voltage. Therefore executing SEIG under balanced resistive load and the balanced excitation, the voltage and the stator currents, load currents and the currents of the capacitors are balanced. In this case, the voltage buildup is quite fast. Therefore, in a specific load margin, a SEIG can be effective, and inexpensive as a system for feeding of isolated areas, even when loads are unbalanced, regardless of whether static converters are used.

References

[1]   B. Multon, O. Gergaud, H. B. Ahmed, X. Roboam, S. Astier, B. Dakyo, *et al.*, "Etat de l'art dans les aérogénérateurs électriques," *Rapport de sysnthèse: l'électronique de puissance vecteur d'optimisation pour les énergies renouvelables», Club Electronique de Puissance,* 2002.

[2]   F. F. El-Sousy, M. Orabi, and H. Godah, "Maximum power point tracking control scheme for grid connected variable speed wind driven self-excited induction generator," *Journal of Power Electronics,* vol. 6, pp. 52-66, 2006.

[3]   J.-F. Yhuel, "Commande en courant des machines à courant alternatif," ANRT [diff.], 2001.

[4]   A. M. Bouzid, A. Cheriti, P. Sicard, M. Bouhamida, and M. Benghanem, "State space modeling and performance analysis of self-excited induction generators for wind simulation," in *Control, Engineering & Information Technology (CEIT), 2015 3rd International Conference on*, 2015, pp. 1-6.

[5]   B. EL MOUBAREK, "RÉGULATION DE LA TENSION D UNE GÉNÉRATRICE ASYNCHRONE AUTO EXCITÉE EN UTILISANT UN COMPENSATEUR STATIQUE D ÉNERGIE RÉACTIVE," Ecole Nationale Polytechnique d'Oran, 2012.

[6]   D. Guérette, *Asservissement d'une éolienne à vitesse variable et à pas fixe dans le cadre d'un système de jumelage éolien-diesel à haute pénétration*: Université du Québec à Rimouski, 2010.

[7]   C. Grantham and D. Seyoum, "The dynamic characteristics of an isolated self-excited induction generator driven by a wind turbine," in *Electrical Machines and Systems, 2008. ICEMS 2008. International Conference on*, 2008, pp. 2351-2356.

[8]   D. Seyoum, C. Grantham, and M. F. Rahman, "The dynamic characteristics of an isolated self-excited induction generator driven by a wind turbine," *Industry Applications, IEEE Transactions on,* vol. 39, pp. 936-944, 2003.

[9]   M. S. Abdoulaziz, "Etude du Générateur Asynchrone pour l'utilisation dans la production de l'énergie éolienne," *Mémoire d'ingénieure Ecole Nationale Polytechnique d'Alger,* 2007.

[10]   A. M. Bouzid, P. Sicard, A. Cheriti, J. M. Guerrero, M. Bouhamida, and M. S. Golsorkhi, "Voltage and frequency control of wind-powered islanded microgrids based on induction generator and STATCOM," in *Control, Engineering & Information Technology (CEIT), 2015 3rd International Conference on*, 2015, pp. 1-6.

[11]   D. Lubineau, "Commande non linéaire de moteur asynchrone avec observateur," 1999.